RSC Advances

PAPER

View Article Online
View Journal | View Issue

Cite this: *RSC Adv.*, 2021, **11**, 35408

Facile and large-scale synthesis of polymorphic graphdiyne catalyzed by transition metal salts for organic pollutant removal†

Jianhui Zhu,[a] Desheng Liu,[a] Changsheng Li,[ab] Bingjie Zhang,[a] Jianli Wang,[a] Wenjuan Wu,[a] Jiawen Ji[a] and Yongqiang Ma *[a]

Received 4th September 2021
Accepted 21st October 2021

DOI: 10.1039/d1ra06653f

rsc.li/rsc-advances

Organic pollutants widely exist in the environment, causing a lot of potential harm. On account of excellent physical and chemical properties, graphdiyne (GDY) has been widely used in many potential fields. However, it is crucial to develop more synthetic methods to achieve mass production of GDY and explore its universality in the removal of organic pollutants. Herein, six transition metal salts including Cu salts and Pd salts were selected as catalysts to successfully synthesize GDY with different morphologies by a coupling reaction. The method is simple, safe, easy to operate and suitable for large-scale production. Among them, $CuSO_4$-catalyzed GDY has higher yield (>90%), lower density and fewer defects. Furthermore, it can efficiently remove organic pollutants from water such as dyes, tetracycline antibiotics and neonicotinoid pesticides, demonstrating that the adsorption material has a certain universality. In particular, the adsorption effect of GDY on dye is comparable to that of MWCNTs and stronger than that of conventional adsorbents such as graphene and activated carbon. This work provides more possibilities for the industrial production of GDY and its promising application for the removal of organic pollutants.

Introduction

Graphdiyne (GDY, the chemical structure as shown in Fig. 1) is composed of a 2,4-hexadiyne carbon chain (–C≡C–C≡C–) connected with benzene rings, and is a new carbon allotrope after fullerene, carbon nanotubes and graphene.[1–7] It not only has 2D monolayer flat material characteristics similar to graphene such as good electrical conductivity and large specific surface area, but also has 3D porous material properties.[8–10] Thus, GDY has promising application prospects in many fields, such as catalysis,[11–15] sensing and detection materials,[16–18] gas separation,[19,20] lithium or energy storage,[13,21–23] water purification,[24–26] *etc.* However, the research on GDY is still mainly at the laboratory stage, and there will be huge space to develop more synthesis methods to realize mass production for more potential applications.

The synthesis of GDY depends on the dimerization reaction of acetylene. It was not prepared until 2010 *via* an *in situ* Glaser coupling reaction on a copper substrate by Prof. Yuliang Li's group, laying the foundation for experimental research on the GDY material.[27] Since then, a series of synthesis methods have been developed, and meanwhile GDYs with various morphologies have been obtained. The common methods of GDY synthesis are currently carried out on a variety of templates such as graphene, diatomite, glass, anodic aluminum oxide, copper nanowire, *etc.*11,28–31 In addition, some researchers also prepared GDY by interface methods or chemical vapor deposition (CVD),[32–34] which is difficult and complex to preprocess the template and separate the GDY from the template-GDY compound. And mass production will be time-consuming and costly in actual production. For special reaction conditions like explosion method, the reaction time is greatly shortened, but side reactions are easy to occur and there are certain safety risks.[35] As a consequence, it is necessary to develop a safe, simple, low-cost method suitable for large-scale production.

Based on the above, we developed a method for direct preparation of GDY in precursor hexaethynylbenzene (HEB) and

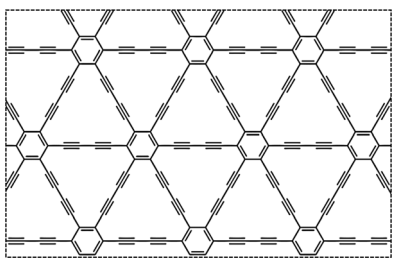

Fig. 1 Chemical structure of graphdiyne (GDY).

[a]*Department of Applied Chemistry, College of Science, China Agricultural University, Beijing, 100193, China. E-mail: mayongqiang@cau.edu.cn*

[b]*Engineering Research Center of Plant Growth Regulator, Ministry of Education & College of Agronomy and Biotechnology, China Agricultural University, Beijing, 100193, China*

† Electronic supplementary information (ESI) available. See DOI: 10.1039/d1ra06653f

pyridine solution using transition metal salts as catalyst. Transition metal salts catalyzed coupling reactions have always been an active field.[36–38] GDY catalyzed by palladium compounds has not been reported up to now, and powdered copper salts are rarely reported to directly synthesize GDY in solution. Herein, six transition metal compounds including cuprous(I) chloride (CuCl), cuprous(I) iodide (CuI), cupric(II) acetate monohydrate ($Cu(OAc)_2$), copper(II) sulfate ($CuSO_4$), palladium(II) acetate ($Pd(OAc)_2$) and bis(triphenylphosphine) palladium(II) chloride ($[(C_6H_5)_3P]_2 \cdot PdCl_2$) were selected as catalysts to synthesize GDYs. The GDYs with different morphologies, crystallinity and defects were obtained by means of SEM, Raman, IR, XPS and other characterization methods, then the growth time of GDY with the highest quality was optimized. This method is simple, safe, high yield and takes less time than such conventional methods, which can also realize large-scale preparation. Besides, the removal of organic pollutants including dye, tetracycline antibiotics and neonicotinoid pesticides in water by GDY in practical application has been carried out. The results indicate that GDY can effectively adsorbate and remove organic pollutants from water, which is a potential and universally applicable absorbent material.

Experimental section

Reagents and materials

Tetrabutylammonium fluoride (TBAF (1 M in THF)), tetracycline antibiotics, rhodamine B (RhB) and methyl orange (MO) were obtained by J&K Chemicals (Beijing, China). Bis(triphenylphosphine) palladium(II) chloride, palladium(II) acetate and tetrakis(triphenylphosphine)-palladium(0) are purchased from Energy Chemical (Shanghai, China). Cuprous(I) chloride, cuprous(I) iodide and cupric (II) acetate monohydrate were from Aladdin (Shanghai, China). Multiwalled carbon nanotubes (MWCNTs) was bought from Pioneer Nanotechnology Co. (Nanjing, China) and reduced graphene oxide (RGO) was synthesized by ourselves according to the Hummers' method. *N*-Propyl ethylene diamine (PSA), graphitized carbon black (GCB), octadecyl silane (C18) and florisil were obtained from Agela Technologies (Tianjin). Except these, other reagents and materials were supplied by Sinopharm Chemical Reagent Co., Ltd. (Shanghai, China). All chemical reagents were used directly in this experiment without further purification.

Materials characterization

Scanning electron microscope (SEM, Hitachi SU8020, Japan) and transmission electron microscope (TEM, FEI Talos F200X) was used to observe the surface morphology and structure of the synthetic materials. The Energy Dispersive Spectrometer (EDS, HORIBA EX-350, Japan) was applied to analyze the types and content of the elements in the micro zone, together with the use of SEM. Besides, Raman spectra (Renishaw inVia) were recorded at the room temperature with a 532 nm laser to characterize GDYs mentioned. Fourier transform infrared spectroscopy (FTIR, PerkinElmer 2000, America) was performed to analyze the surface functional groups of those by squashing method with the scanning range from 400 to 4000 cm^{-1}. Meanwhile, X-ray diffraction (XRD, Brucker D8 Advance, Germany) was carried out on the pyrolyzed samples with a powder diffractometer with Cu/Ka radiation measurements. X-ray photoelectron spectroscopy (XPS, Thermo escalab 250Xi, America) was measured to analyze and infer the possible presence of elements and their chemical state. What's more, the Zeta (Zetasizer Nano ZS90, America) potential analysis of the GDY surface in an aqueous solution was carried out.

Synthesis of graphdiyne (GDY) powder

GDY was synthesized *via* an acetylenic coupling reaction of HEB (see the ESI† for the specific synthesis process of HEB).

Different catalysts to synthesize GDY. 100 mL pyridine and one of the transition metal salt catalysts including CuCl, CuI, $Cu(OAc)_2$, $CuSO_4$, $Cu(OAc)_2$, $[(C_6H_5)_3P]_2 \cdot PdCl_2$ were added to a three-port flask and stirred thoroughly in advance, respectively. Successively, the concentrated deprotected HEB was dissolved in 40 mL pyridine, transferred to a constant pressure drop funnel, and slowly dropped for 12 h into above solution under nitrogen protection at 60 °C. The mixture was stirred at 60 °C for 2 days and then cooled down approximately room temperature, washed with *N*,*N*-dimethylformamide, purified water and acetone in turn to remove monomers and oligomers. Finally, the prepared material was dried overnight at 65 °C.

Different growth time to synthesize GDY. After screening out the best catalyst, the same steps above were used to respectively synthesize GDY at different growth times including 1 day, 1.5 days and 2 days. Black brownish GDY powders prepared under different conditions were obtained.

Dye adsorption test

The absorbances of RhB and MO with different concentrations (20 mg L^{-1}, 10 mg L^{-1}, 5 mg L^{-1}, 1 mg L^{-1}, 0.5 mg L^{-1} and 0.01 mg L^{-1}) were measured to obtain standard curves of RhB and MO respectively. Then, the adsorption effect of the above GDYs synthesized under different catalysts and different growth time were compared with other seven common adsorbents including MWCNTs, RGO, GCB, activated carbon (AC), PSA, C18 and Florisil. Detailed Experimental methods were shown in ESI.†

The absorbances of the above solutions were measured by UV-Vis fractional photometer, and the values obtained at the maximum absorption wavelength (RhB: λ_{max} = 554 nm; MO: λ_{max} = 464 nm) were converted to concentration through a standard curve. The removal efficiency (RE) of each adsorbent material was calculated separately by the following formula:

$$\mathrm{RE}\ (\%) = \frac{C_0 - C_1}{C_0} \times 100\%$$

where C_0 (mg L^{-1}) and C_1 (mg L^{-1}) refer to the concentration of RhB or MO before and after adsorption, respectively.

Other organic pollutants adsorption test

To verify the adsorption performance of GDY, four tetracycline antibiotics (oxytetracycline, doxycycline, tetracycline and chlorotetracycline) and five neonicotinoid pesticides (acetamiprid, clothianidin, thiacloprid, imidacloprid and

nitenpyram) were tested. The concentration of the adsorption material GDY and the above mixed solution in centrifuge tubes was 1 g L^{-1} and 2 mg L^{-1}, respectively, which was oscillated at a speed of 170 rpm for 2 h until equilibrium was reached. All samples were analyzed by HPLC-MS/MS (Agilent Technologies, USA) equipped with an Agilent 1200 HPLC series and an Agilent 6410B triple-quadrupole mass spectrometer.

Results and discussion

Effect of different catalysts on the morphology of GDYs

Scanning electron microscope (SEM) was used to observe the morphology of GDY powders. Abundant structural information of materials can be obtained by transmission electron microscope (TEM) testing. It can be seen from the Fig. 2, S3 and S4† that there are some differences in the morphology of GDY synthesized by different catalysts. Fig. 2(a) and S4(a)† show that the CuCl-catalyzed GDY is formed by the aggregation of many regular shaped nanospheres with a diameter of about 100 nm. And the distribution of pores is formed during the aggregation process of the nanospheres. CuI-catalyzed GDY still maintains the porous structure on the whole, which is composed of nanometer microspheres with snowflake crystal shape, with a smaller diameter (Fig. 2(b) and S4(b)†). The low-magnification SEM as shown in Fig. S3(c)† indicates that the GDY catalyzed by $Cu(OAc)_2$ is a solid powder in bulk with a certain thickness, and there are many folds and small holes on the surface, which are more obvious at high magnifications (Fig. 2(c)). TEM image (Fig. S4(c)†) shows that the GDY synthesized by $Cu(OAc)_2$ catalyst is also composed of many nanospheres, with a diameter of about 15 nm. The GDY obtained by $CuSO_4$ catalyst not only maintains a certain lamellar structure, but also has a rough, loose and porous surface (Fig. 2(d) and S4(d)†). From Fig. 2(e and f), it can be concluded that the GDYs prepared by the two palladium compounds are both made of small particles closely aggregated into large spherical particles with rough surface. TEM images (Fig. S4(e and f)†) further confirm this structure.

Effect of different catalysts on the structure of GDYs

Raman spectroscopy is an effective method to characterize the structure of carbon materials and can be used to determine the bonding structure of GDY. As is demonstrated in the Fig. 3(a), the Raman spectra of the prepared GDY under different catalysts is in accordance with the literature reports.[27,39,40] It can be observed that two very obvious peaks are the D band located at 1378 cm^{-1} and the G band at 1581 cm^{-1}. The former corresponds to the breathing vibration of the sp^2 hybrid carbon atom of the benzene ring and is the disordered band of GDY, whose strength is closely related to the structural defects, and the latter is due to the in-plane stretching vibration of the sp^2 hybrid carbon atom. Hence, the ratios of the intensity of D band to G band of GDY synthesized by different catalysts were acquired, which can be used to evaluate the quality of GDY. It can be summarized from the Fig. 3(c) that the GDY synthesized by CuCl catalyzed has a high content of defects due to its I_D/I_G of 0.86; while for $CuSO_4$-catalyzed GDY, the I_D/I_G of was 0.75, indicating that it is highly ordered and has few defects. Moreover, there are weak peaks at about 1982 cm^{-1} and 2140 cm^{-1}, which are ascribed to the stretching vibration of the C≡C bond in the conjugated diacetylene chains (–C≡C–C≡C–). The structures of the prepared GDYs were further elucidated by FTIR (Fig. 3(d)). The absorption peaks at 1473 cm^{-1} and 1595 cm^{-1} are attributed to the vibration of aromatic ring skeleton, and the weak peak at 2104 cm^{-1} is the stretching vibration of acetylene bond in GDYs.

UV-Vis absorption spectrum as shown in the Fig. S5(a)† were used for analysis their optical properties. The absorption spectrum of materials will be redshifted with the increase of conjugation degree. Compared with the monomer, the absorption of GDYs had obvious redshift and broad absorption band, which explained that the electron delocalization could be enhanced by extending the conjugated π system.[41,42] The bandgap energy of GDYs prepared by different catalysts was estimated by the relationship of $(\alpha h\nu)^{1/2}$ *versus* photo energy (Fig. S5(b)†). Their band gap was about 0.5 eV, which was within the reported range.[28,43] The XRD patterns in the Fig. 3(b) reveal a wide diffraction peak near 23° correspond to a weaker crystallinity of the prepared GDYs.

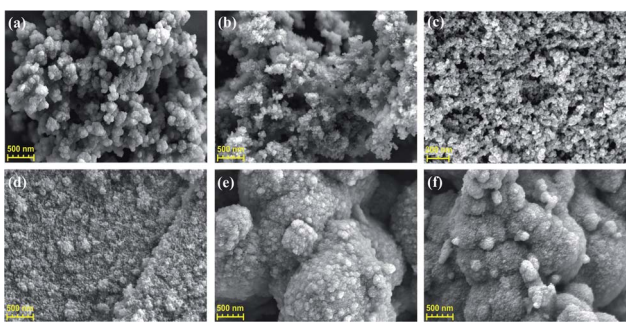

Fig. 2 SEM images of GDY synthesized by different catalysts. Scale bar is 500 nm. Catalyst: (a) CuCl; (b) CuI; (c) $Cu(OAc)_2$; (d) $CuSO_4$; (e) $Pd(OAc)_2$; (f) $[(C_6H_5)_3P]_2 \cdot PdCl_2$.

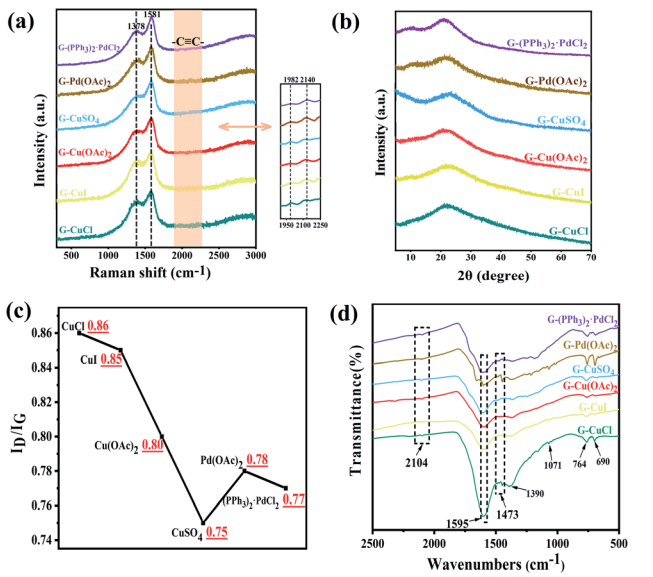

Fig. 3 Characterizations of GDY synthesized by different catalysts. (a) Raman spectra; (b) XRD patterns; (c) ratio of the intensity of D band to G band in Raman; (d) FTIR spectra.

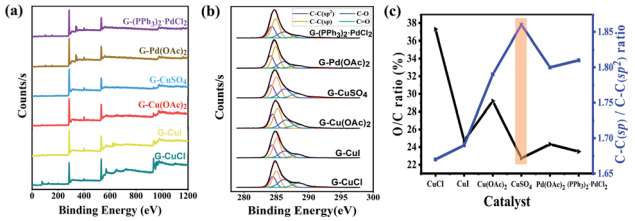

Fig. 4 Characterizations of GDY synthesized by different catalysts. (a) XPS survey scan; (b) C1s XPS; (c) O/C ratio and C–C (sp)/C–C (sp^2) ratio in XPS.

Effect of different catalysts on the composition of GDYs

The composition of GDY and the bonding between atoms were analyzed by X-ray photoelectron spectroscopy (XPS) given in Fig. 4(a), which shows that six synthesized GDYs consist mainly of elemental carbon, with a small amount of oxygen. Oxygen may come from the fact that a little air will be absorbed by GDY itself, or a little end-acetylene at the defect will be oxidized to the oxygen-containing functional groups such as hydroxyl (–OH) or carboxyl (–COOH). The C1s peak at 284.8 eV corresponds to binding energies for the C1s orbital, which was further researched, as illustrated in Fig. 4(b). The C1s spectrum of GDY can be mainly divided and fitted into four sub-peaks at 284.4, 285.1, 286.7 and 288.5 eV, which have been represented to a C1s orbital of C–C (sp^2), C–C (sp), C–O and C=O, respectively.[27,44] And according to the integral result, C–C (sp) is about twice as much as C–C (sp^2), which is basically satisfied with the chemical bond structure of GDY. In other words, there are two acetylene bonds between each benzene ring. The O/C ratio and C–C (sp)/C–C (sp^2) ratio obtained by XPS further revealed that the GDY synthesized by different catalysts had different defect degrees (shown in Fig. 4(c)). It could be seen that there were fewer impurities and vacancies exist in the $CuSO_4$-catalyzed GDY due to its lower O/C ratio (22.74%) and higher C–C (sp)/C–C (sp^2) ratio (1.86), which was corresponding to the above Raman analysis results.

Effect of different growth time on GDYs

In view of the advantages of higher yield (more than 90%, as shown in Fig. 5(a)), lower density, larger volume (about 2–6 times of other GDYs in Fig. 5(b)) and fewer defects of GDY catalyzed by $CuSO_4$, it was chosen to investigate the quality of GDY synthesized at different growth time (1 day, 1.5 days, 2 days).

It can be observed from the SEM and TEM that the GDYs synthesized at the above three growth time are lamellar on the whole. However, closer inspection GDY with growth time of one day (Fig. 6(a)) only forms intermittent and small-size lamellar structures, which becomes more continuous and larger in size with the extension of growth time. In addition, it is obvious that there are many folds on the surface and the edges are warped when the growth time is 1.5 days (Fig. 2(b) and S6(b)†). While at 2 days, the surface is rough and there are many raised particles and concave holes (Fig. 2(d) and S4(d)†). Therefore, it could be inferred that the increase of growth time is conducive to the formation of large area of lamellar structures, but also leads to more defects. According to Fig. 6(c), the Energy Dispersive Spectrometer (EDS) reflects that with the increase of growth time, the proportion of oxygen element increases, which is easier to form defects.

Raman spectra shows that there are also four peaks at 1380 cm^{-1} (D band), 1578 cm^{-1} (G band), 1956 cm^{-1} and 2163 cm^{-1} (Fig. 6(d)). The illustration inside shows the ratio of D band intensity to G band intensity at different growth time, which reveals that the I_D/I_G ratio increases with the increasing growth time of GDY, indicating that the defects of GDY are increasing slightly. XRD spectra in Fig. 6(e) shows that the GDYs synthesized at these three time are amorphous structure.

XPS was performed to explore the structure and elemental composition of the materials, and the results (Fig. 6(f)) were consistent with the EDS analysis, which consists mainly of the element carbon, with a small amount of oxygen. As illustrated in Fig. S7,† the O/C ratio was the lowest when the growth time was 1 day. C 1s spectrum was formed from four subpeaks, sp^2 C–C of benzene rings at 284.5 eV, sp C–C at 285.2 eV, C–O at 286.9 eV, and C=O at 288.5 eV (Fig. S8†). In addition, the ratio of C–C (sp)/C–C (sp^2) was close to 2 at these three time, and the value reached the maximum when the growth time was 1 day, indicating that the impurities and defects contained were the least, which further confirmed the above analysis.

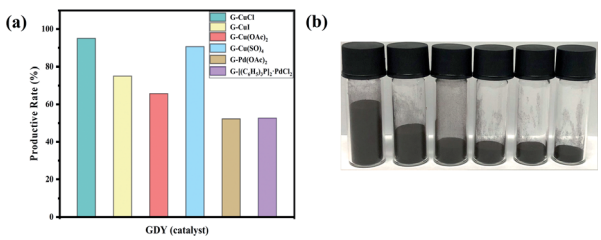

Fig. 5 (a) The productive rate of GDY synthesized by the same mass precursors under different catalysts; (b) sample diagram of GDY synthesized by different catalysts at the same mass. From left to right: $CuSO_4$, CuCl, CuI, $Pd(OAc)_2$, $[(C_6H_5)_3P]_2 \cdot PdCl_2$, $Cu(OAc)_2$.

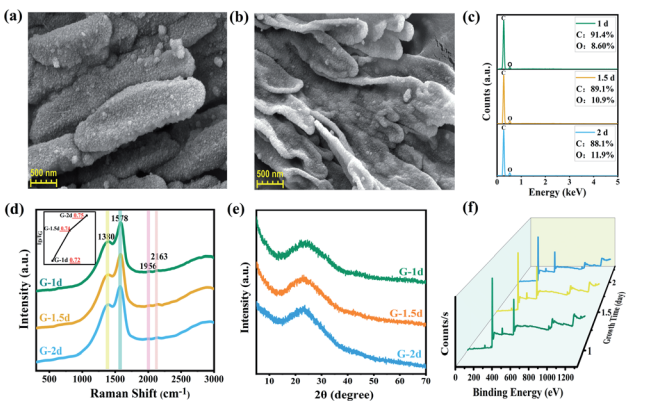

Fig. 6 Characterizations of GDY synthesized at different growth time. SEM images: (a) 1 day and (b) 1.5 days; (c) EDS spectrum. (d) Raman spectra. Inset: ratio of the intensity of D band to G band. (e) XRD patterns. (f) XPS survey scan.

Removal of organic pollutants in water

In recent years, with the rapid development of industry, the harm of organic pollutants including antibiotics, pesticides, dyes and so on to human health and even ecosystem has been widely concerned.[45] Adsorption is considered to be one of the most competitive and commonly used methods due to its low cost, simple operation, wide application range and no by-product generation in the treatment process.[46,47]

In this study, the application prospect of GDY in the removal of dyes from water was researched. The cationic dye rhodamine B (RhB) and the anionic dye methyl orange (MO) were selected to evaluate the adsorption performance of the materials. As shown in the Fig. 7(a), the absorbance–concentration curves are highly linear at concentrations of 0.01–20 mg L^{-1} of RhB and MO, and the determination coefficients (R^2) are greater than 0.999, which can be used for the subsequent conversion between the absorbance value and concentration. The GDYs synthesized by different catalysts adsorbed RhB and MO dyes in aqueous solution, respectively. The adsorption experiments showed in Fig. 7(b) that the removal effect of the GDYs synthesized by copper salts was obviously better than those by palladium salts. Moreover, the removal efficiency of $CuSO_4$-catalyzed GDY in copper salts was the best. It was inferred that the difference of dyes adsorption effect may be caused by the surface structure, *etc.* There were holes, folds and voids on the surface of GDYs catalyzed by copper salts, which were more conducive to the attachment of dye molecules.

In addition, under the condition of $CuSO_4$ catalysis, GDY synthesized at different growth time adsorbed RhB and MO respectively, and on the whole they both have good adsorption effect for two dyes (Fig. 7(c)). The adsorption performance for cationic dye RhB was similar, which could reach more than 98%. However, for the anionic dye MO, there were some differences. When the growth time was 1 day, the adsorption efficiency of GDY (close to 95%) was slightly better than those of GDYs growing for 1.5 days and 2 days (about 85%). For understanding the main factor of the difference between the removal effect of anionic and cationic dyes, zeta potential measurement was carried out. It was found from the Table S1† that the surface potentials of the synthesized GDYs at three growth time were all negative. Due to their mutual attraction with cationic dyes, they all had good effects. But at one day, the repulsive force between GDY and anionic dyes was smaller than the other two growth time, thus adsorption efficiency in growth time of 1 day was higher. As can be seen qualitatively from Fig. 7(e), when $CuSO_4$-catalyzed GDY with growth time of 1 day, the color of the supernatant of RhB and MO was almost colorless, which also confirmed its good adsorption effect.

The aforementioned GDY with the best adsorption effect was compared with the seven common adsorbents MWCNTs, RGO, GCB, AC, PSA, C18 and Florisil for the adsorption of RhB and MO. As illustrated in Fig. 7(d) and (f), the adsorption capacity of GDY for both RhB and MO was much higher than that of the other six adsorbents except MWCNTs. There's no obvious difference between the GDY and MWCNTs. However, the preparation method of GDY was simpler and less energy consumption than that of MWCNTs in the production process. All these results demonstrate that GDY is a promising adsorbent material for removing dye pollution from water efficiently and quickly.

Moreover, in order to explore the universality of GDY in the removal of organic pollutants, tetracycline antibiotics and neonicotinoid pesticides were further investigated as representative substances. As shown in Fig. 8, GDY had a certain adsorption effect on both types of organic pollutants, in which the removal efficiency of tetracycline antibiotics reached more than 80% (Fig. 8(a)). GDY has different degrees of removal effects for different pollutants, indicating that it is a kind of

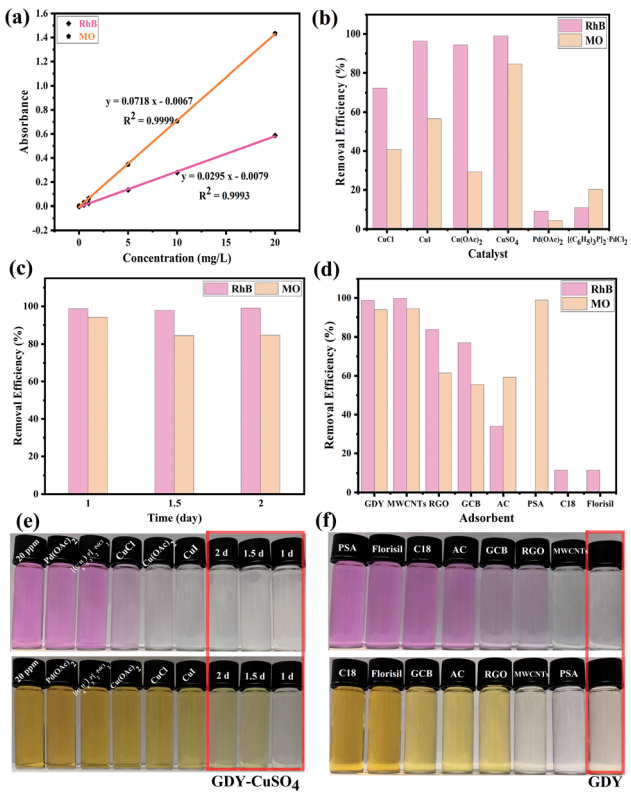

Fig. 7 (a) Standard curves of absorbance *versus* concentration of RhB and MO; removal efficiency for adsorption of RhB and MO: (b) GDY synthesized by different catalysts; (c) GDY catalyzed by $CuSO_4$ at different growth time; (d) contrast with conventional adsorbents. Color of RhB and MO supernatant after adsorption. (e) GDYs of different synthesis methods; (f) conventional adsorbents.

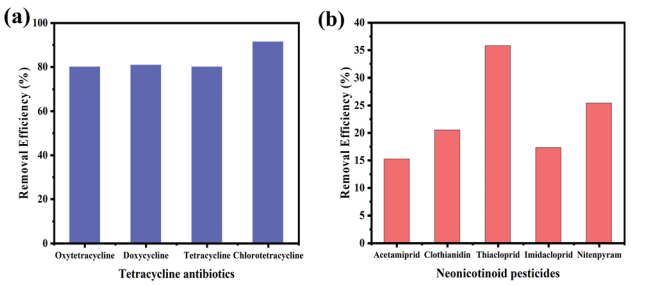

Fig. 8 Adsorption effect of GDY on different organic pollutants. (a) Tetracycline antibiotics; (b) Neonicotinoid pesticides.

adsorption material with great potential and has universal application.

Conclusions

In conclusion, GDY powders with different morphologies were successfully prepared by coupling reaction of precursor HEB with different transition salts catalysts including copper salts, palladium salts and different growth time with 1 day, 1.5 days and 2 days. This method is carried out under mild conditions and eliminates the restriction of template, which makes the synthesis process more simple, safe, low-cost, and can be produced on a large scale in the industrial. The GDYs prepared by copper salt have many loose structures such as pores and folds, while the surface of those synthesized by palladium salt is more compact. Among them, $CuSO_4$ catalyzed GDY has fewer defects and higher yield. In addition, adsorption experiments prove that this material can be widely applied in the removal of organic pollutants. Especially, it can quickly and efficiently remove dyes from water and its adsorption effect is comparable to that of MWCNTs and stronger than that of graphene and activated carbon. Therefore, GDY can be acted as a potential adsorbent for the removal of pollutants in the water environment. Furthermore, the GDYs obtained by this synthetic method provide possibilities for the development of applications in more fields.

Conflicts of interest

There are no conflicts to declare.

Acknowledgements

This work was supported by The National Key Research and Development Program of China (2016YFD0201203).

Notes and references

1 Y. Li, L. Xu, H. Liu and Y. Li, *Chem. Soc. Rev.*, 2014, **43**, 2572–2586.
2 C. Huang, Y. Li, N. Wang, Y. Xue, Z. Zuo, H. Liu and Y. Li, *Chem. Rev.*, 2018, **118**, 7744–7803.
3 Y. Xue, B. Huang, Y. Yi, Y. Guo, Z. Zuo, Y. Li, Z. Jia, H. Liu and Y. Li, *Nat. Commun.*, 2018, **9**, 1460.
4 Z. Jia, Y. Li, Z. Zuo, H. Liu, C. Huang and Y. Li, *Acc. Chem. Res.*, 2017, **50**, 2470–2478.
5 W. Krätschmer, L. D. Lamb, K. Fostiropoulos and D. R. Huffman, *Nature*, 1990, **347**, 354–358.
6 S. Lijima, *Nature*, 1991, **354**, 56–58.
7 K. S. Novoselov, A. K. Geim, S. V. Morozov, D. Jiang, Y. Zhang, S. V. Dubonos, I. V. Grigorieva and A. A. Firsov, *Science*, 2004, **306**, 666–669.
8 Z. Zuo and Y. Li, *Joule*, 2019, **3**, 899–903.
9 E. M. Dakota, F. Teresa, A. H. Todd and O. P. Richard, *Nat. Commun.*, 2018, **9**, 1.
10 A. Fasolino, J. H. Los and M. I. Katsnelson, *Nat. Mater.*, 2007, **6**, 858–861.
11 J. Li, J. Xu, Z. Xie, X. Gao, J. Zhou, Y. Xiong, C. Chen, J. Zhang and Z. Liu, *Adv. Mater.*, 2018, **30**, 1800548.
12 L. Hui, Y. Xue, H. Yu, Y. Liu, Y. Fang, C. Xing, B. Huang and Y. Li, *J. Am. Chem. Soc.*, 2019, **141**, 10677–10683.
13 Y. Du, W. Zhou, J. Gao, X. Pan and Y. Li, *Acc. Chem. Res.*, 2020, **53**, 459–469.
14 Y. Lv, X. Wu, W. Jia, J. Guo, H. Zhang, H. Liu, D. Jia and F. Tong, *Carbon*, 2020, **169**, 45–54.
15 Y. Fang, Y. Xue, L. Hui, H. Yu and Y. Li, *Angew. Chem., Int. Ed.*, 2021, **60**, 3170–3174.
16 Y. Li, X. Li, Y. Meng and X. Hun, *Biosens. Bioelectron.*, 2019, **130**, 269–275.
17 Y. Li, H. Huang, R. Cui, D. Wang, Z. Yin, D. Wang, L. Zheng, J. Zhang, Y. Zhao, H. Yuan, J. Dong, X. Guo and B. Sun, *Sens. Actuators, B*, 2021, **332**, 129519.
18 L. Wu, J. Gao, X. Lu, C. Huang, Dhanjai and J. Chen, *Carbon*, 2020, **156**, 568–575.
19 Y. Jiao, A. Du, M. Hankel, Z. Zhu, V. Rudolph and S. C. Smith, *Chem. Commun.*, 2011, **47**, 11843–11845.
20 S. W. Cranford and M. J. Buehler, *Nanoscale*, 2012, **4**, 4587–4593.
21 Y. Lin, H. Kang, M. Liang, X. Ye, J. Li, Q. Feng, Y. Zheng and Z. Huang, *Appl. Surf. Sci.*, 2020, **526**, 146457.
22 T. Lu, J. He, R. Li, K. Wang, Z. Yang, X. Shen, Y. Li, J. Xiao and C. Huang, *Energy Storage Mater.*, 2020, **29**, 131–139.
23 Y. Yue, Y. Xu, F. Kong, Q. Li and S. Ren, *Carbon*, 2020, **167**, 202–208.
24 S. Lin and M. J. Buehler, *Nanoscale*, 2013, **5**, 11801–11807.
25 R. Liu, J. Zhou, X. Gao, J. Li, Z. Xie, Z. Li, S. Zhang, L. Tong, J. Zhang and Z. Liu, *Adv. Electron. Mater.*, 2017, **3**, 1700122.
26 J. Li, Y. Chen, J. Gao, Z. Zuo, Y. Li, H. Liu and Y. Li, *ACS Appl. Mater. Interfaces*, 2019, **11**, 2591–2598.
27 G. Li, Y. Li, H. Liu, Y. Guo, Y. Li and D. Zhu, *Chem. Commun.*, 2010, **46**, 3256–3258.
28 X. Gao, Y. Zhu, D. Yi, J. Zhou, S. Zhang, C. Yin, F. Ding, S. Zhang, X. Yi, J. Wang, L. Tong, Y. Han, Z. Liu and J. Zhang, *Sci. Adv.*, 2018, **4**, eaat6378.
29 F. Zhao, N. Wang, M. Zhang, A. Sapi, J. Yu, X. Li, W. Cui, Z. Yang and C. Huang, *Chem. Commun.*, 2018, **54**, 6004–6007.
30 G. Li, Y. Li, X. Qian, H. Liu, H. Lin, N. Chen and Y. Li, *J. Phys. Chem. C*, 2011, **115**, 2611–2615.
31 H. Shang, Z. Zuo, L. Li, F. Wang, H. Liu, Y. Li and Y. Li, *Angew. Chem., Int. Ed.*, 2018, **57**, 774–778.
32 R. Matsuoka, R. Sakamoto, K. Hoshiko, S. Sasaki, H. Masunaga, K. Nagashio and H. Nishihara, *J. Am. Chem. Soc.*, 2017, **139**, 3145–3152.
33 C. Yin, J. Li, T. Li, Y. Yu, Y. Kong, P. Gao, H. Peng, L. Tong and J. Zhang, *Adv. Funct. Mater.*, 2020, **30**, 2001396.
34 R. Liu, X. Gao, J. Zhou, H. Xu, Z. Li, S. Zhang, Z. Xie, J. Zhang and Z. Liu, *Adv. Mater.*, 2017, **29**, 1604665.
35 Z. Zuo, H. Shang, Y. Chen, J. Li, H. Liu, Y. Li and Y. Li, *Chem. Commun.*, 2017, **53**, 8074–8077.
36 S. Chen, W. Wu and F. Tsai, *Green Chem.*, 2009, **11**, 269–274.
37 A. Bakhoda, O. E. Okoromoba, C. Greene, M. R. Boroujeni, J. A. Bertke and T. H. Warren, *J. Am. Chem. Soc.*, 2020, **142**, 18483–18490.

38 R. Schmidt, R. Thorwirth, T. Szuppa, A. Stolle, B. Ondruschka and H. Hopf, *Chem.–Eur. J.*, 2011, **17**, 8129–8138.
39 K. Xiao, J. Li, X. Wu, H. Liu, C. Huang and Y. Li, *Carbon*, 2019, **144**, 72–80.
40 J. Ding, S. Shi, H. Zhao, P. Liu and H. Yu, *Carbon*, 2021, **176**, 235–241.
41 G. Luo, X. Qian, H. Liu, R. Qin, J. Zhou, L. Li, Z. Gao, E. Wang, W. Mei, J. Lu, Y. Li and S. Nagase, *Phys. Rev. B*, 2011, **84**, 075439.
42 J. Zhou, X. Gao, R. Liu, Z. Xie, J. Yang, S. Zhang, G. Zhang, H. Liu, Y. Li, J. Zhang and Z. Liu, *J. Am. Chem. Soc.*, 2015, **137**, 7596–7599.
43 Q. Zheng, G. Luo, Q. Liu, R. Quhe, J. Zheng, K. Tang, Z. Gao, S. Nagase and J. Lu, *Nanoscale*, 2012, **4**, 3990–3996.
44 S. Zhang, H. Liu, C. Huang, G. Cui and Y. Li, *Chem. Commun.*, 2015, **51**, 1834–1837.
45 P. Manvendra, K. Rahul, K. Kamal, M. Todd, U. P. Charles and M. Dinesh, *Chem. Rev.*, 2019, **119**, 3510–3673.
46 F. Suo, G. Xie, J. Zhang, J. Li, C. Li, X. Liu, Y. Zhang, Y. Ma and M. Ji, *RSC Adv.*, 2018, **8**, 7735–7743.
47 Z. Tang, X. Hu, H. Ding, Z. Li, R. Liang and G. Sun, *J. Colloid Interface Sci.*, 2021, **594**, 54–63.